Power Management of Hybrid Flywheel-Battery Energy Storage Systems Considering the State of Charge and Power Ramp Rate

Seyede Masoome Maroufi, *Student Member, IEEE,* Shahab Karrari, Karthik Rajashekaraiah, *Student Member, IEEE,* Giovanni De Carne, *Senior Member, IEEE*

***Abstract*—A flywheel and lithium-ion battery's complementary power and energy characteristics offer grid services with an enhanced power response, energy capacity, and cycling capability with a prolonged system lifetime. Real-time Power management and considering storage components' State of Charge (SoC) and ramp rate are crucial for optimizing performance. However, there is a need for further improvements in SoC correction techniques and rigorous, realistic testing to ensure accurate and efficient management strategies. This paper proposes a Moving Average (MA) and Fuzzy Logic-based power management for a Hybrid Flywheel and Battery Energy Storage System that optimally share the power among the two technologies, considering the flywheel's SoC and the battery's ramp rate as the most concerning variable of each technology. The system minimizes SoC and ramp rate imbalances by integrating Moving Averages for dynamic energy demand adjustments and Fuzzy Logic controllers for efficient power redistribution. A Power Hardware-in-the-Loop (PHIL) experimental validation utilizing a 120 kW, 7.2 kWh flywheel-based energy storage system coupled with a simulated battery demonstrates improved SoC correction and ramp rate management performance.**

***Index Terms*—Hybrid energy storage, power management, State of Charge, ramp rate, flywheels**

I. Introduction

THE increasing power variability generated by intermittent renewable energy production and load consumption (e.g., electric vehicles) calls for integrating fast dynamic energy storage systems (ESS) such as batteries, flywheels, and supercapacitors [1], [2]. Among these, batteries are widely used for their high energy density, allowing for effective storage and release of large energy quantities [3]. However, fast power cycling can significantly reduce battery life [4]. On the other hand, high-power storage technologies such as supercapacitors and Flywheel Energy Storage Systems (FESS) have high power density and rapid response capabilities with no major lifetime concerns [5]–[8].

Flywheels are advantageous for delivering power for several minutes compared to supercapacitors, which provide energy for only tens of seconds. Flywheels store kinetic energy through high-speed rotor spinning, making them ideal for applications requiring frequent, fast energy exchanges [6], [9]. Notable industrial applications include the Beacon 20 MW Power flywheel plant in New York for grid frequency regulation [10], Schwungrad's 150 kW plant in Ireland for fast stabilization services [11], and Amber Kinetics' systems in the Philippines for grid stability and renewable energy integration with a four-hour discharge duration [12]. These examples demonstrate flywheels' ability to improve energy efficiency, response times, and lifespan despite lower energy density [6], [13].

No single ESS meets all performance criteria, so Hybrid Energy Storage Systems (HESS) are often used to combine the strengths of different technologies [14], [15]. However, this can increase control complexity. In HESS, combined power and energy management is crucial for optimal power distribution across technologies. Focusing only on power may deplete fast dynamic ESS, reducing system flexibility. Thus, the State of Charge (SoC) is a key indicator of stored energy and must be considered. Accurate SoC estimation improves system dynamics and efficiency and extends component lifespan by minimizing abrupt state changes [16], [17].

The battery's ramp rate is crucial for HESS control, influencing its ability to manage power quality and frequency demands. For voltage sags, the ESS must inject power quickly (1–10 minutes) and ramp to peak power without exceeding its discharge capacity. In frequency control, the ESS must respond within 30 seconds for primary control and sustain power for up to 20 minutes for secondary control [18], [19]. Moreover, the ramp rate impacts battery lifespan, as rapid power changes increase currents and extreme states of charge, accelerating degradation over time [20]. By controlling charging limits and reducing the frequency of large cycles and surges, battery lifespan can more than double [16], [21], [22]. Therefore, the ramp rate is essential for operational efficiency and prolonging the battery's life, making it a critical parameter for the HESS's performance and sustainability.

Some recent advancements in energy management and SoC for HESS are as follows. While some studies [23], [24] focus on power management, others also address SoC control [25]–[29], primarily in HESS with supercapacitors. Flywheel technology, however, offers advantages over supercapacitors, such as higher energy density and simpler construction [30], making it a promising choice for enhancing energy storage systems [31], [32].

Progress in controlling FESS includes the tube-based MPC

Masoome Seyed Maroufi, Karthik Rajashekaraiah, and Giovanni De Carne are with the Institute for Technical Physics, Karlsruhe Institute of Technology, Germany. Shahab Karrari is with Siemens Energy, Erlangen, Germany. The work of Masoome Seyede Maroufi, Karthik Rajashekaraiah, and Giovanni De Carne has been supported by the Helmholtz Association under the program "Energy System Design" and under the Helmholtz Young Investigator Group "Hybrid Networks" (VH-NG-1613).

approach for handling disturbances [8], addressing frequency and voltage fluctuations [33], and an adaptive droop control for frequency changes [34]. These works focus on single systems, overlooking HESS integration.

The work in [35] introduces a fuzzy logic-based power smoothing control for a HESS with a flywheel and lead-acid battery, optimizing power distribution. While the battery's SoC is actively managed, the flywheel's SoC is not addressed, risking rapid discharge and delayed recovery.

The study in [36] introduces two control strategies for a HESS in an electric shipboard microgrid, combining batteries and flywheels. The first, an optimization-based approach, aims to minimize energy losses, while the second uses a lookup table for efficiency. Both effectively manage load fluctuations in simulations but highlight areas for improvement regarding the flywheel's SoC. The optimization strategy overlooks SoC, leading to inefficient flywheel use, while the lookup-table approach lacks real-time SoC tracking, risking overcharging or discharging. Notably, these valuable studies have yet to undertake experimental validation with an actual FESS of their proposed controllers within real-world environments. All the aforementioned contributions and their research efforts have been summarized in Table I.

To address proper power and energy management for HESS, this paper introduces a controller that combines fuzzy logic and moving average techniques to optimize power and energy set-points of different ESS technologies. The controller considers the power rate of change in a high-energy density storage device (i.e., battery) and the SoC of a high-power energy storage device (i.e., flywheel) as controlled variables. Fuzzy logic control (FLC) is chosen for power-sharing control due to its flexibility and intuition in determining the average window of the moving average, enhancing adaptability to changing conditions (SoC and ramp rate) [37]. Unlike other methods, this integrated controller enables direct control over the flywheel's output power and SoC, optimizing the overall system performance.

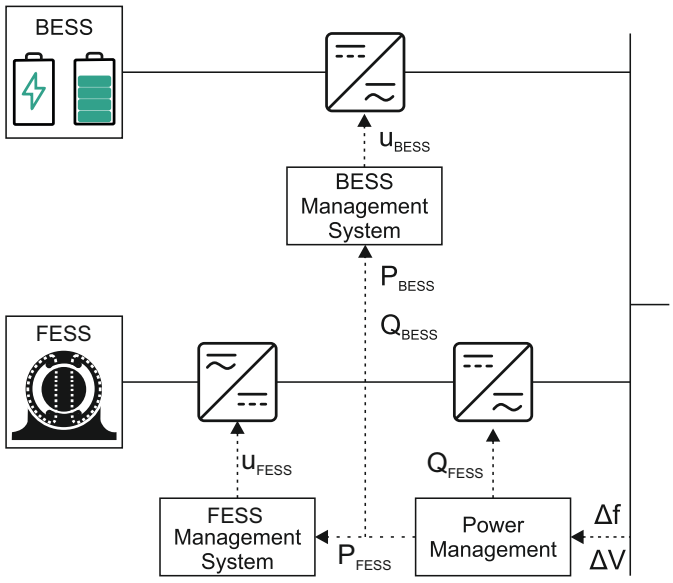

Fig. 1: General HESS management system architecture

Figure 1 illustrates the overall HESS structure consisting of a battery and a flywheel in the grid. Figure 1 illustrates a power management example for HESS. In this diagram, the power management system responds to frequency and voltage contingencies (Δf and ΔV) by assigning active and reactive power (P and Q) reference values to each storage system and its converters. Each device's management system then communicates the necessary control signals to ensure efficient regulation of its operations. In our study, this distribution is based on two main control requirements: the battery's ramp rate and the flywheel's SoC.

The proposed controller optimizes the HESS trade-off between power and SoC management. While prioritizing power management enhances performance, it may limit availability for a longer duration. By controlling the SoC, the HESS can remain available for additional power events, expanding its intervention capabilities. This novel approach is compared to classical techniques based on low-pass filters in a PHIL experimental setup with a 120 kW commercial FESS, demonstrating the potential for broader integration into future energy systems.

To summarize, the paper introduces the following novel contributions:

- A novel energy and power management approach for HESS based on moving average and fuzzy logic has been proposed that distributes optimally the power set-points between the battery and the flywheel.
- Implemented a fuzzy logic control approach to effectively monitor the flywheel's SoC and make informed decisions about power contributions from a FESS, ensuring optimized system performance.
- The proposed control strategy is designed to manage a HESS by splitting the power between storage elements in an optimal way, specifically aiming to minimize fast power variations directed to the batteries, and avoiding low SoC for FESS.
- The proposed approach has been validated experimentally in realistic grid conditions using a commercial 120kW 7.2kWh high-speed flywheel by means of Power Hardware In the Loop testing. This kind of validation has never been carried out for flywheel-based HESS.

The rest of this paper is structured as outlined below: Section II elaborates on the design of the suggested controller. Section III outlines the practical validation of the proposed control approach, and Section IV provides a parameter variation analysis of the chosen tuning values. Finally, Section V concludes the paper.

II. Proposed Control Strategy

This section presents the methodology employed for the controller and power management of an HESS, which consists of a battery and flywheel. Figure 2 shows the overall control scheme, divided into three main parts: a) The first part involves the power signal separation using a moving average block. The moving average smooths out short-term fluctuations in the data and highlights longer-term trends. In this case, it helps to separate the power signal into components, dividing

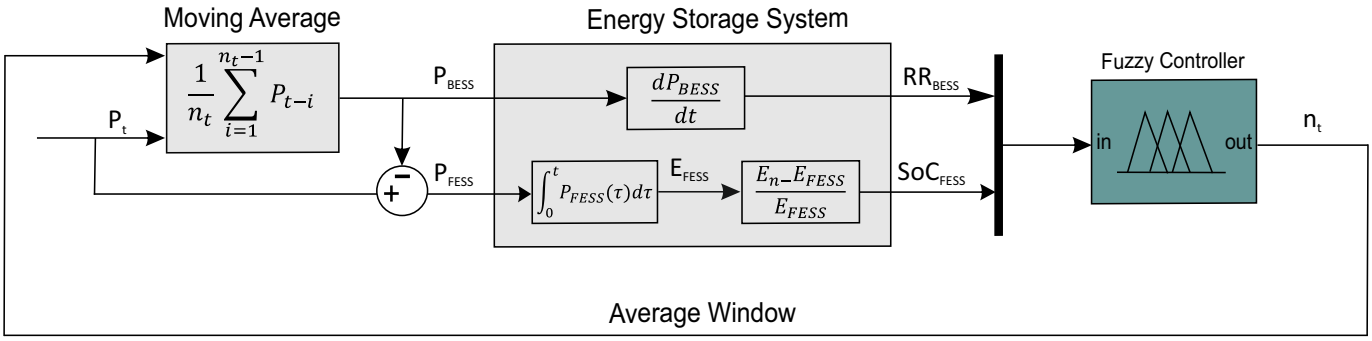

Fig. 2: Control scheme for HESS including the moving average and fuzzy logic stages

the fast-changing components and the slower ones. This is crucial for the next step, where the battery and flywheel handle these different components based on their unique capabilities; *b*) The second part determines the ramp rate of the battery and SoC of the flywheel with the calculated power output. Ramp rate refers to how quickly the battery can charge or discharge power without causing excessive wear. In this step, the ramp rate of the battery is calculated based on its power, ensuring that it is not subjected to abrupt changes that could reduce its lifespan. On the other hand, the flywheel's SoC ensures that it stays within the appropriate operating limits. The flywheel handles fast power changes due to its mechanical energy storage properties, making it ideal for smoothing out quick variations in power demand. Based on the SOC, the system calculates how much power the flywheel should absorb or release. The SoC of the flywheel is calculated based on the energy integrated from its power.; *c*). The third part is followed by applying a Fuzzy Logic Controller (FLC) to determine the average window of the moving average. This process separates the input power profile into two distinct components: one representing the fast response for the FESS and the other representing the slow response for the BESS. By utilizing FLC, the control system can effectively manage and regulate the SoC levels of the FESS, ensuring that it is maintained within the desired operating range and the rate of change of power in the battery to help its longevity. Subsequently, a detailed description of each of these steps is provided.

A. Moving Average

A moving average involves calculating the average of consecutive values in a time series, obtained through mathematical convolution [38]. Widely used in finance, particularly in the Moving Average Strategy (MAS), it aids in monitoring price trends and identifying potential reversals in securities [39], [40]. MAS generates buy or sell signals by evaluating the disparity between long-term and short-term averages. Beyond finance, moving averages find application in load forecasting, power quality analysis, and filtering in power systems.

TABLE I: State of the art on hybrid energy storage systems

Reference	Objective	HESS		ESS Type	Control		Setup	
		HESS	Flywheel		SoC	RR[a]	RTS[b]	PHIL[c]
[23]	Decrease power rating of the converter	✓	✗	BESS-UC	✗	✗	✗	✗
[24]	Voltage regulation	✓	✗	BESS-SC	✗	✗	✓	✗
[25]	Increase BESS Lifetime	✓	✗	BESS-SC	✓	✗	✗	✗
[26]	Control power distribution	✓	✗	BESS-UC-Fuel cell	✓	✗	✗	✗
[27]	Power sharing	✓	✗	BESS-SC	✓	✗	✗	✗
[28]	Power fluctuations	✓	✗	BESS-SC	✓	✗	✗	✗
[29]	Supply uninterrupted power	✓	✗	multiple ESDs	✓	✗	✓	✗
[8]	Voltage regulation	✗	✓	FESS	✗	✗	✓	✗
[33]	Frequency control	✗	✓	FESS	✗	✗	✓	✗
[34]	Frequency control	✗	✓	FESS	✓	✗	✓	✓
[35]	Power fluctuations	✓	✓	lead acid BESS-FESS	✓	✗	✗	✗
[36]	Power fluctuations	✓	✓	BESS-FESS	✓	✗	✓	✗
This paper	Energy management	✓	✓	BESS-FESS	✓	✓	✓	✓

✓= investigated ✗= not investigated

[a]Considered ramp rate of battery
[b]Used real-time simulation
[c]Used power hardware in the loop

In this context, moving average filters are employed to discern the behavior of two energy storage systems. The filter characterizes the gradual behavior of elements like batteries, while the differential value highlights rapid fluctuations in faster energy storage, exemplified by flywheels. The Simple Moving Average (SMA) is defined as follows:

$$\mathrm{SMA}(t) = \frac{1}{n_t} \sum_{i=1}^{n_t-1} P_{t-i} \tag{1}$$

Variable n_t indicates the length of the period over time. Variable P indicates the data points, and t is the point we need to calculate.

By using the MAS, the BESS effectively manages the gradual changes, while the Fast FESS addresses the rapid changes within the HESS.

B. Fuzzy Logic Controller

In this study, the optimization of power and energy set-points for different ESSs, particularly the interaction between the BESS and FESS, is a key focus. The Fuzzy Logic Controller (FLC) is designed to dynamically balance these systems using the BESS ramp rate and the FESS's SoC as inputs. The controller's output is the average window length of the moving average filter, which helps manage the power flow between the two storage systems. As mentioned in the introduction, this work includes the limitations of the BESS ramp rate and FESS SoC in the control strategy. For this reason, the FLC is designed to determine the average window of the moving average filter, which allows a good trade-off between power control and SoC management.

1) Membership Functions: Rather than representing the inputs and outputs using specific values, the fuzzy sets describe the inputs and outputs by incorporating linguistic terms and flexible reasoning. The precise inputs and outputs are transformed into fuzzy sets defined by membership functions. In this paper, the ramp rate of the BESS and the SoC of the FESS are the inputs of the FLC. On the other hand, the average window length of the moving average filter is the controller's output. Figure 3 shows the membership functions of the inputs and the output while the definition of the fuzzy sets in linguistic terms are defined in table II.

In this research, the Matlab/Simulink implementation of Mamdani's fuzzy inference method is chosen as it is widely utilized as the standard fuzzy methodology in control systems [41], [42]. The ramp rate and SoC membership functions are divided into low and high categories based on each ESS's benefits. The ramp rate and SoC membership functions are categorized into low and high for two primary reasons: simplicity and relevance to the specific energy management strategy for our HESS. By focusing on these two categories, we are able to streamline the decision-making process, ensuring that the fuzzy logic controller can quickly and effectively adjust the power management strategy. Additionally, in our specific application, the most critical factors are when the ramp rate is too high (causing stress on the system) and when the SoC is either too low (risking depletion) or too high (to maximize system efficiency). Expanding the categories beyond these two does not significantly enhance control performance but would increase computational complexity. Maintaining a flywheel SoC above 30% is imperative, as the mechanical rotational mass is crucial for optimal performance. A SoC below this threshold results in reduced speed, compromising the flywheel's ability to deliver maximum power when required. Although high SoC is not harmful to FESS, the SoC membership function for FESS is divided into two categories for the better performance of HESS when the SoC of the FESS and ramp rate of the BESS are both high.

The average window is divided into four categories to better balance power management. Trapezoidal membership functions are used for the ramp rate and SoC, providing smooth transitions between low and high values, while triangular membership functions are applied to the average window, enabling more focused control over power flow adjustments. The fuzzy logic methodology allows the system to continuously fine-tune the output (average window length) based on real-time conditions, thus optimizing the power exchange between the two storage systems. Table III represents the range of each input and output membership function.

2) Rules of Fuzzy Controller: The FLC is centered around its rule base, which comprises decision-making rules. Each rule consists of an antecedent (current system state using fuzzy sets and variables) and a consequent (desired action/output).

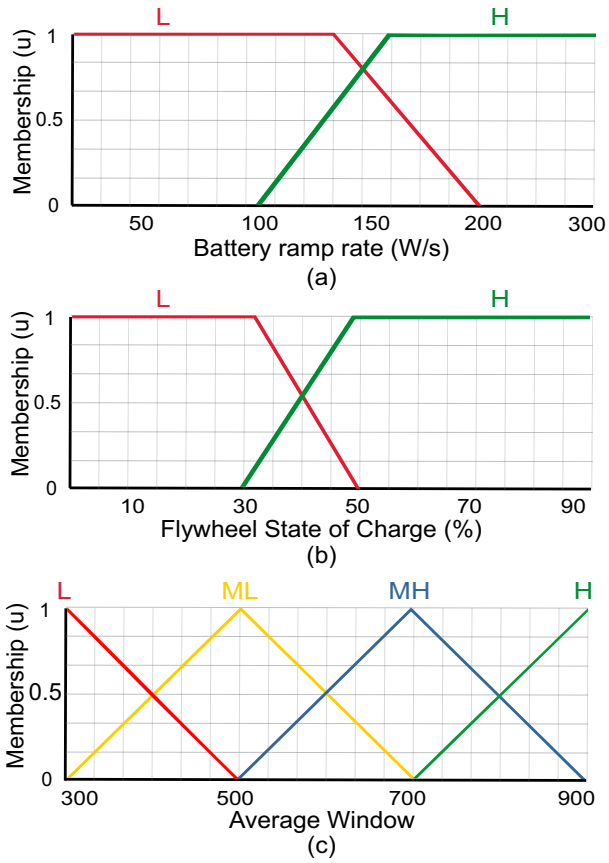

Fig. 3: Membership Functions (a) Battery Energy Storage Ramp Rate (b) Flywheel Energy Storage State of Charge (c) Average window of Moving Average

Fuzzy sets and variables define the conditions and outputs of the rules. The overall system output results from combining multiple rule inputs/outputs. The system's complexity and control requirements determine the number of rules and linguistic variables. FLCs, with their added flexibility and precision, effectively handle complex and uncertain systems. In our specific case, Table IV illustrates the rules of the FLC. For example, in scenarios where the battery ramp rate is low, and the SoC of the flywheel is concurrently depleted, minimizing the average window of the moving average can prioritize using battery resources for power management. In contrast, when the flywheel's SoC is high, and the battery ramp rate is high, the FLC directs more power to be utilized from the flywheel, allowing the flywheel to compensate for the high battery ramp rate. This balances the system by using the flywheel's higher energy reserve. The rules in Table IV allow the FLC to continuously adjust the power distribution between the BESS and FESS based on the current conditions, ensuring a dynamic and efficient power management strategy. By defining these fuzzy sets, the system can make informed decisions on balancing the energy storage resources depending on the state of the two systems.

III. Experimental Validation

In this study, the control analyses play a crucial role in governing the operation of a HESS to match a power profile obtained from reference [43]. This power profile is derived using an enhanced motif discovery algorithm, identifying the most recurrent daily consumption patterns within the target time series with a 1 s time step. The input data utilized for the analyses were gathered in South Germany during the summer of 2018, collected from four distinct 10/0.4 kV substations. The data was collected during this period to ensure a high level of PV generation is captured in the sizing analysis. The four substations were selected based on their relative voltage sensitivity to changes in active power according to the method proposed in [44]. The data was recorded at various resolutions, starting from 1 second, using the "PQI-DA Smart" measurement device from A-Eberle [45]. This device was installed on the low-voltage side of the substation transformer to measure the total power from all feeders connected to each substation and to assist in sizing a centralized ESS. Given the high resolution of the data and limited storage capacity, two weeks of data were collected at each substation. By harnessing this dataset and discerning the dominant consumption patterns, the control analyses aim to regulate the behavior of the HESS, aligning it with the energy requirements represented by the identified power profile.

TABLE II: Fuzzy sets and their linguistic variables

Sets	Linguistic Variables
L	Low
ML	Medium Low
MH	Medium Low
H	High

Figure 4 illustrates the separation of the input power when the moving average is over 10 minutes. For this specific input data, the moving average output is in the range of ± 160 kW, and the difference between the input and output of the moving average filter is in the range of ± 30 kW.

A. Hardware Under the Test (HUT)

To empirically confirm the effectiveness of the suggested control approach, the controller is applied to an actual 120 kW, 7.2 kWh high-speed FESS. The configuration of the FESS is shown in fig 5, which consists of a flywheel or high inertia rotor, a Permanent Magnet Synchronous Motor (PMSM), a back-to-back bi-directional power converter with a common DC link, and auxiliary components required for running the system. Furthermore, fig 6 displays the internal perspective of the commercial FESS container.

B. Power Hardware-in-the-Loop Setup

This paper's experimental validation uses a Power Hardware-in-the-Loop (PHIL) setup, integrating theoretical precision with real-world hardware interactions. The implementation involves integrating a controller based on the combination of moving average and fuzzy logic. Figure 7 illustrates a schematic diagram of the setup created to assess the performance of the proposed control design.

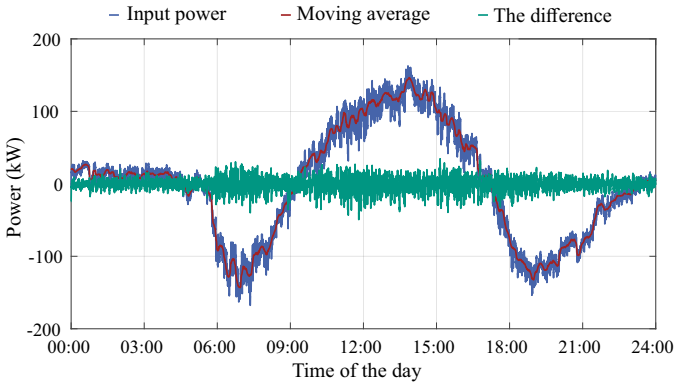

Fig. 4: The profile of the input power, the moving average filter, and the difference between them

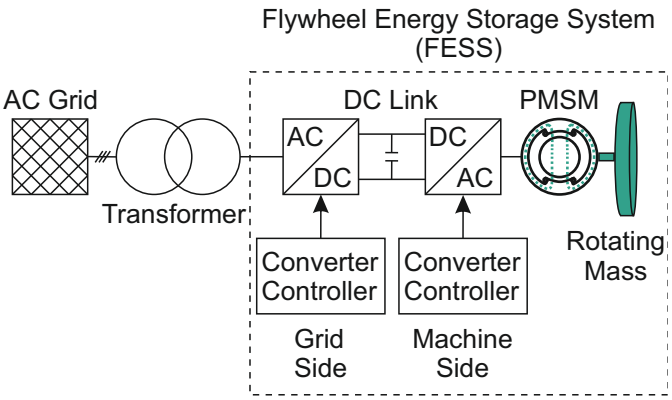

Fig. 5: Configuration of a Flywheel Storage System

TABLE IV: Rules of fuzzy logic controller

		Flywheel SoC	
		L	**H**
Battery Ramp Rate	**L**	L	MH
	H	MH	H

The setup consists of three main parts. The simulated part in the real-time simulator, the actual device, and the communications and connections between these two parts. Opal-RT OP5700 real-time simulator simulates the proposed control in real-time. The controller controls the input power mentioned in section II integrated into a low-voltage microgrid and generates the active power references for both the BESS and FESS. The active power reference of BESS is sent to the battery model within the real-time simulator. For the parameters to be controlled, the SoC of the flywheel is obtained by the device, while the ramp rate (RR) of the battery is derived from its power as shown in equation (2) in the simulation environment.

In the battery model, the nominal capacity E_n is crucial in determining the number of cells in a Li-ion battery and the maximum rotational speed and inertia in a flywheel. Calculating the nominal capacity involves integrating the power profile of the ESS and assessing the maximum change in resulting energy variations, as outlined in equations (3) and (4). However, in efforts to prolong the lifespan of an ESS, especially in the context of Li-ion batteries, it is expected to employ oversizing. For Li-ion batteries, research has indicated that steering clear of high SoC values can significantly mitigate the cells' cathode degradation and calendar aging. Likewise, deep discharging has been shown to elevate the internal resistance of the cells [46]. Consequently, allocating a specific non-usable capacity is advisable to prevent extreme SoC values, denoted as SoC_{min} and SoC_{max}. Thus, the nominal capacity can be determined by considering the minimum and maximum SoC, assuming 10% and 90%, respectively. The round trip efficiency of the battery (η) is assumed to be 90%.

Fig. 6: Inside view of the container holding the two 60 kW Stornetic high-speed FESS.

$$RR = \frac{dP(t)}{dt}. \tag{2}$$

$$E(t) = \eta^{-sgn(P(t))} \int_0^t P(\tau)\, d\tau, \tag{3}$$

$$E_n = \frac{maxE(t) - minE(t)}{SoC_{max} - SoC_{min}}. \tag{4}$$

The FESS terminal grid voltages are also simulated and transmitted to a 400 kVA-switch-mode power amplifier by EGSTON Power Electronics. The connection between the FESS and the amplifier utilizes a Small-Factor pluggable (SFP) connection, employing Xilinx's Aurora protocol. The power amplifier has the capability to both supply power to and absorb power from the FESS. The FESS currents are measured at the connection point using DQ640ID-B Danisense current transformers. These measured currents are then forwarded to an Opal-RT OP4510 I/O extension box, which employs another SFP connection to send the data to the real-time simulator, effectively closing the loop. The ideal transformer method facilitates the interface between the FESS and the real-time simulation. This method is widely used in practical PHIL simulations due to its simplicity and standardization [47]–[49]. The voltages at the FESS terminal are also measured and sent back to the real-time simulator. However, these voltage measurements are solely utilized for calculating the FESS power within the simulator and do not play a role in the PHIL interfacing algorithm.

The proposed controller requires knowledge of the BESS's ramp rate and the FESS's SoC. The ramp rate of the battery is calculated from its power derivative in its model presented in the real-time simulator. FESS's SoC, measured internally

TABLE III: Membership functions sets and their range

Battery Ramp Rate (RR)		**Flywheel SoC**		**Average Window (AW)**	
Set	**Range**	**Set**	**Range**	**Set**	**Range**
L	RR<200	L	SoC<50%	L	AW<500
				ML	300<AW<500
H	RR>100	H	SoC>30%	MH	500<AW<900
				H	AW >900

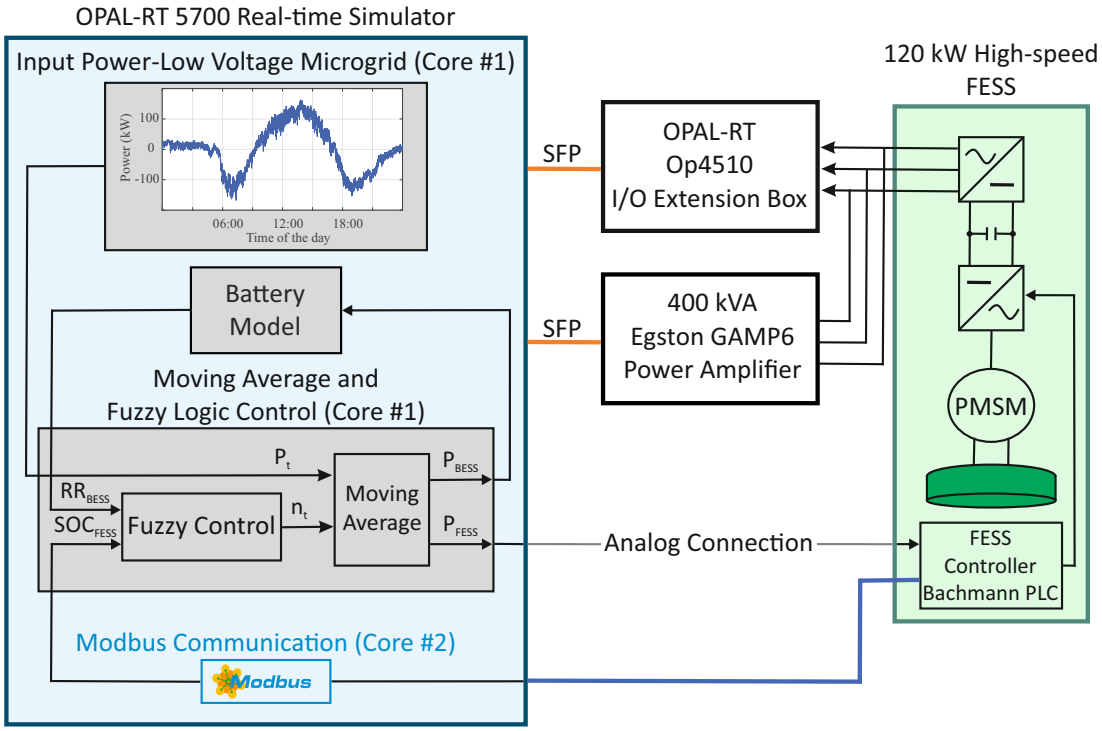

Fig. 7: Setup for prototyping of the proposed controller and PHIL simulation with the 120 kW high-speed FESS.

in the FESS controller, is sent to the real-time simulator using an Ethernet connection and the Modbus TCP/IP protocol from the industrial controller of the FESS.

A dedicated CPU core of the real-time simulator is allocated to manage communication between the FESS industrial controller and the real-time simulator. This dedicated core ensures efficient and reliable communication between the two components.

In this setup, the ethernet connection can transmit reference commands, including the active power reference, to the FESS. However, due to the slow and non-deterministic nature of the Modbus protocol [50], a faster analog signal transmission method is preferred in this particular study. Specifically, a 4-20 mA current signal is used to transmit the active power reference to the FESS, ensuring more efficient and reliable communication.

C. Experimental Results

With the illustrated PHIL setup alongside the FESS, Figure 8 vividly showcases the harmonious correlation between the recorded power output of the FESS and the expected reference power derived from thorough experimental trials. Notably, the depicted curves exhibit a remarkable alignment, showcasing a harmonious synchronization wherein the measured power from the FESS closely shadows the reference power, substantiating a robust correlation between the two. Furthermore, fig 9 demonstrates the change of the average window in the time frame of the experiment.

In this research, we compare our proposed control approach with a low-pass filter (LPF) also used in [27], [28], [31], [35], [51], [52]. A LPF dispatches the power between the battery

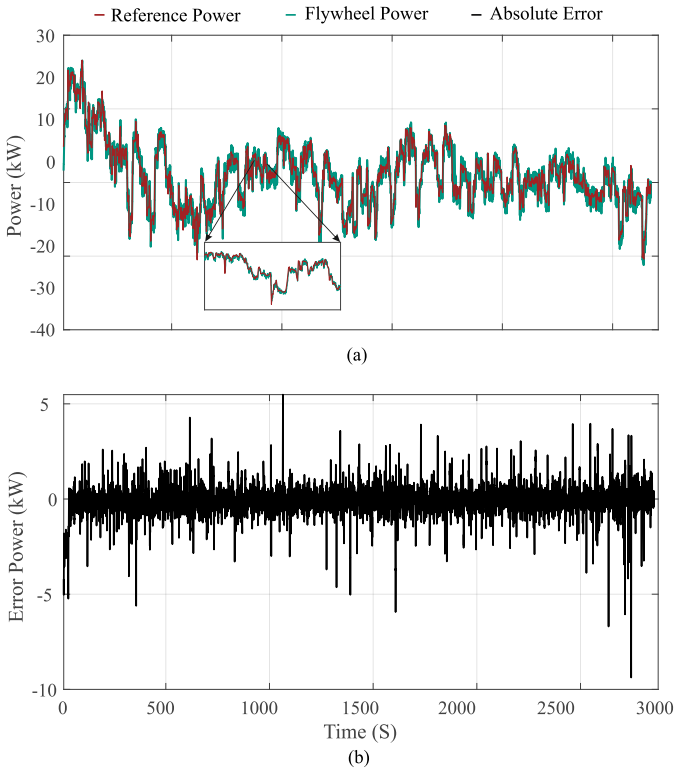

Fig. 8: Comparison between the reference power and the power from the hardware in the flywheel (a) Reference and measured Power (b) Absolute error between the reference and measured power

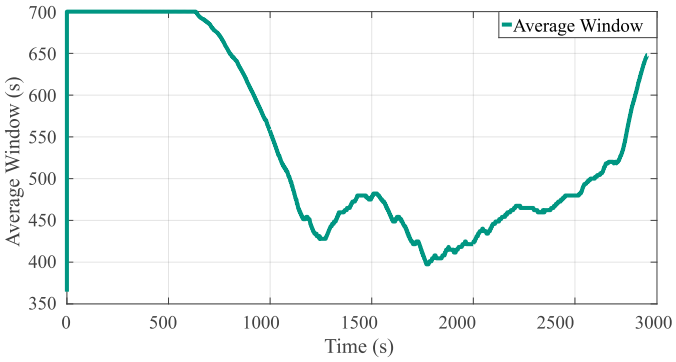

Fig. 9: Average Window of the moving average

and the flywheel, splitting the low and the high-frequency signals based on (5). The overall structure of the controller with a LPF is shown in figure 10.

$$Filter = \frac{1}{1+Ts} \tag{5}$$

with s as Laplace operator and $T = \frac{1}{f_{cut-off}}$, where w_f is the cut-off frequency of the filter. Here a 2.5 mHz cut-off frequency is used for the LPF to satisfy the requirement for the input power with the available HESS. The choice of a 2.5 mHz cut-off frequency for the filter has been made to ensure that the SoC of the energy storage devices remains positive and avoids negative values. We determined this frequency based on the sizes of the two energy storage systems and their dynamics. Figure 11 visually demonstrates how input power is distributed between the BESS and FESS when using the filter method and our new control strategy, which combines moving average and fuzzy logic techniques.

The suggested control strategy allocates input power efficiently to both the BESS and the FESS. Its objective is to reduce the battery's ramp rate while ensuring that the SoC of the flywheel remains consistently above 40%. Figure 12 illustrates how the SoC of the flywheel, obtained from experimental results, is maintained above the 40% threshold with the proposed controller when compared to its fluctuation using the filter method. Notably, the incorporation of fuzzy logic enables us to adapt the averaging window size in a manner that further minimizes the battery's ramp rate which is obtained from the post-analysis of experimental data in figure 12.

It's noteworthy to mention that a basic control strategy using a filter neglects the significant role of the auxiliary power of

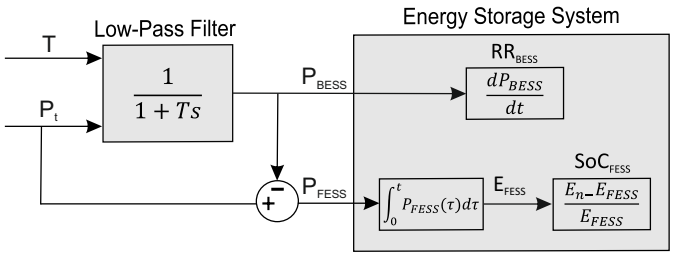

Fig. 10: Control scheme with a low-pass filter

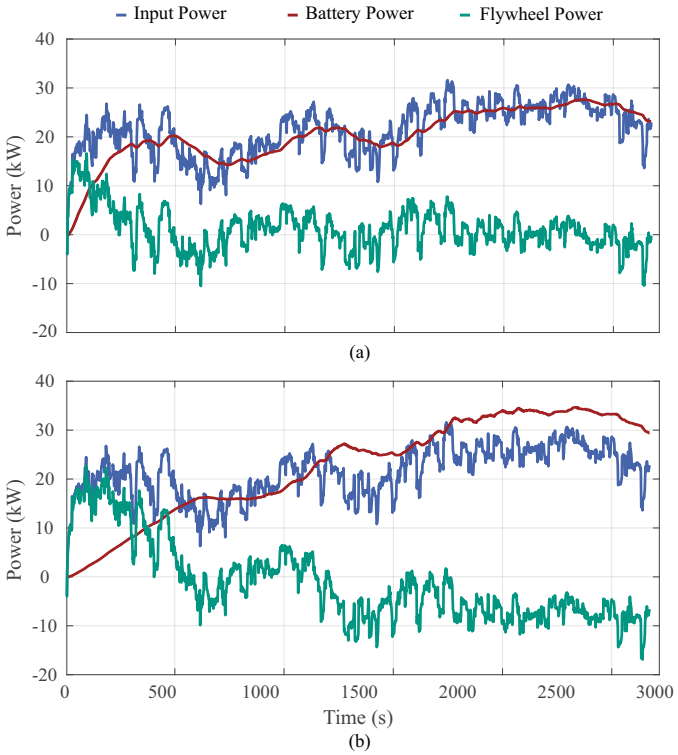

Fig. 11: Experimental comparison of power in two methods (a) Filter method (b) Fuzzy-Moving average Method

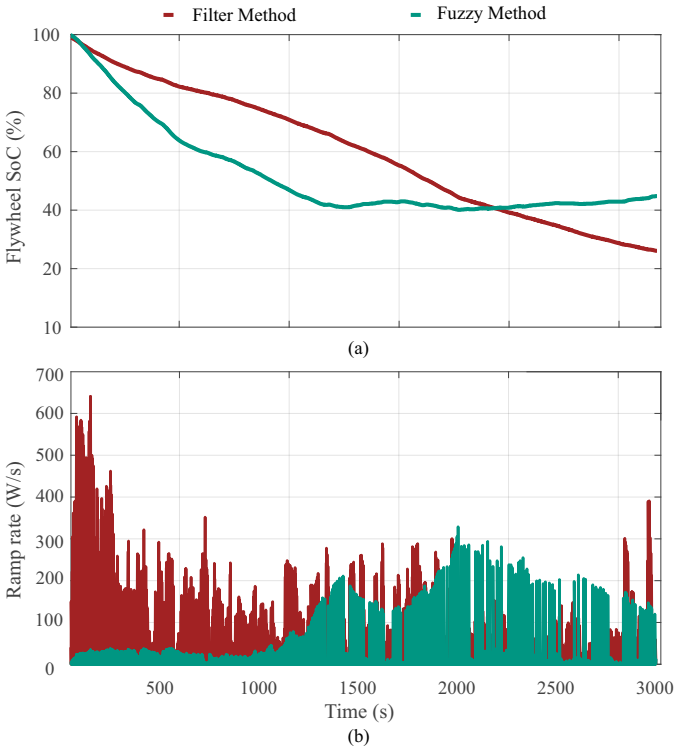

Fig. 12: Comparison of the Filter Method and the Fuzzy-Moving average method (a) Flywheel SoC from experimental results (b) Battery ramp rate derived from post-analysis of experimental data

the flywheel. When working with an actual flywheel system, this auxiliary power becomes a dynamic factor that varies depending on the device's SoC. By incorporating control over the SoC, we ensure that this auxiliary power is appropriately taken into account. Furthermore, it is essential to recognize that when the SoC of the flywheel drops below 30%, the maximum power capacity of the flywheel cannot be fully utilized. This limitation leads to a quicker depletion of the flywheel's energy reserves.

IV. Parameter Variation Analysis

Fuzzy logic algorithms are characterized by the needs of humans' inputs for their parameter settings. However, a different parameter tuning may vary the optimization results, affecting the performance of the proposed algorithm. For this reason, in this work we have performed a parameter variation analysis of the moving average window width in the fuzzy logic controller and the cut-off frequency in the low-pass filter, showing why specific parameters have been adopted in the previous experimental results.

A. Moving Average Window Width

The selection of the moving average window width is a critical factor influencing the performance of the HESS. Simulations have been performed using the daily power profile and battery model described in Section III. The primary goal was to achieve a balance between the ramp rate of the BESS and the SoC dynamics of the FESS.

A lower range for the average window length restricts the controller's decision-making flexibility, leading to suboptimal smoothing of the power signal. On the opposite, a higher range can result in operational inefficiencies, with the system responding too frequently to minor fluctuations. Figure 13 illustrates these trade-offs, considering simulations for two window width ranges: 300–900 s (the proposed one) and 100–1300 s (higher range). The results show that increasing the average window length from 300–900 s to 100–1300 s significantly increases the ramp rate of the BESS, potentially affecting its lifetime. This is attributed to the larger window length introducing excessive variability into the moving average calculation. Consequently, the chosen window width strikes a balance, minimizing ramp rate fluctuations while maintaining efficient smoothing for optimal SoC dynamics.

The works in [53]–[55] underline that the parameter acquisition in fuzzy logic systems is often guided by the specific requirements of the target application, reinforcing the validity of our approach to defining parameters based on the system's operational characteristics. To further demonstrate the adaptability of the proposed fuzzy logic controller, we tested the system with two additional power profiles: one scaled to double the existing power profile and another scaled to half of it. For each case, the ramp rate of the power profile changes, necessitating modifications to the membership function and storage sizes to accommodate the altered dynamics.

The results in Figure 14 compare each power profile's ramp rate and SoC behavior with its corresponding filter range. The results confirm that the controller consistently balances the ramp rate and SoC independently from the power profile dynamics.

B. Low-pass Filter Cut-Off Frequency

In addition to the moving average window width, the cut-off frequency of the low-pass controller was analyzed in the

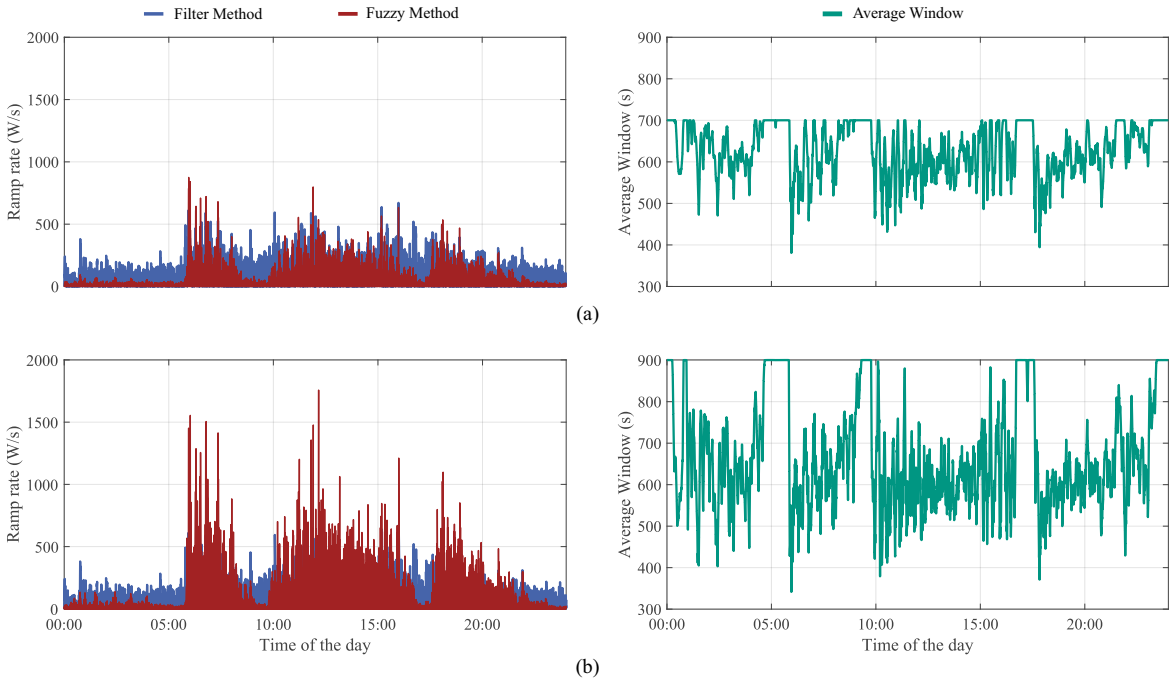

Fig. 13: Effect of different membership functions on the ramp rate and the average window (a) Average window between 300 - 900 s (b) Average window between 100 - 1300 s

same simulation setup. A higher cut-off frequency allows the controller to respond more quickly to fluctuations, improving the SoC dynamics of the FESS by allocating more of the high-frequency power variations to the BESS. However, this comes at the cost of increased ramp rates for the BESS (similarly to the larger moving average window width), as the battery is more exposed to components of the power demand. Conversely, a lower cut-off frequency effectively smooths the BESS ramp rate but compromises the SoC performance. Figure 15 depicts these trade-offs. It can be seen that for the chosen cut-off frequency of 2.5 mHz, the ramp rate of the BESS is comparable with the proposed controller, while the SoC of FESS is kept positive. It also demonstrates how a higher cut-off frequency of 3.5 mHz improves the SoC utilization of the FESS while simultaneously increasing the ramp rate of the BESS. A lower cut-off frequency of 1.5 mHz, on the other hand, achieves the opposite effect of a lower ramp rate of BESS but leads to an empty FESS, highlighting the importance of selecting an intermediate frequency that balances the trade-offs between the parameters.

V. Conclusion

In this paper, we have introduced an innovative power management and control strategy designed for Hybrid Energy Storage Systems (HESS) comprising a Lithium-Ion Battery (LIB) and a Flywheel, with a primary focus on State-of-Charge (SoC) regulation in Flywheel Storage Systems (FESS) while limiting the ramp rate in the power of the battery. Through the integration of Moving Average (MA) and Fuzzy Logic techniques, our approach aims to achieve optimal energy distribution via an adaptive averaging window while simultaneously reducing the ramp rate of the battery and maintaining the SoC of the flywheel.

A comprehensive experimental validation using an actual 120 kW flywheel-based Hybrid Energy Storage System (HESS) prototype has been performed in a Power Hardware-In-The-Loop (PHIL) testing using real-world data (South Germany distribution feeder power measurement). The results show that the proposed approach effectively addresses dynamic load variations. A variable controller based on a Moving Average technique allows for a proactive adjustment in the charging and discharging cycles of individual Energy Storage

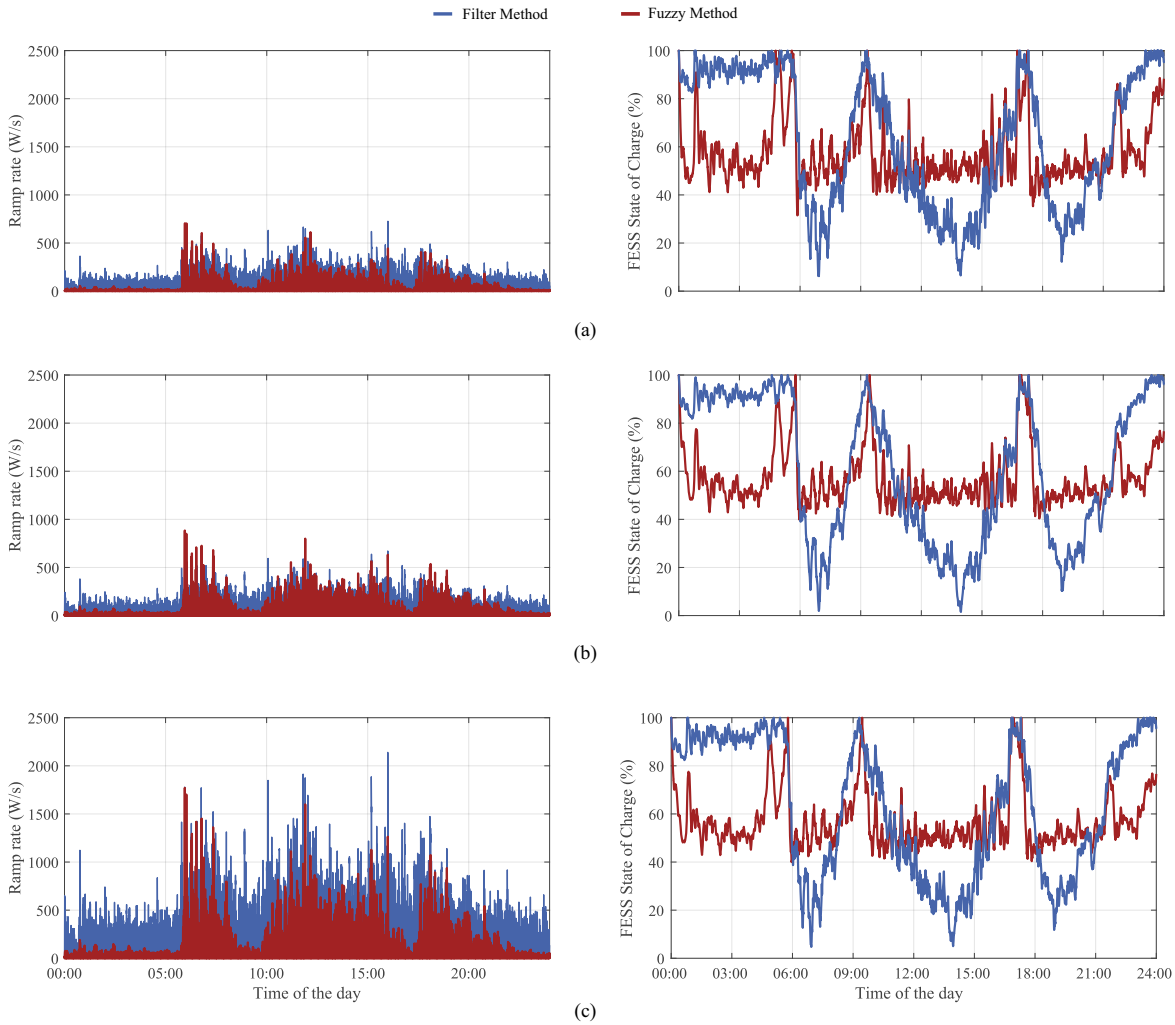

Fig. 14: Comparison of the controller on different power profiles (a) half of the original power profile (b) original power profile (c) twice the original power profile

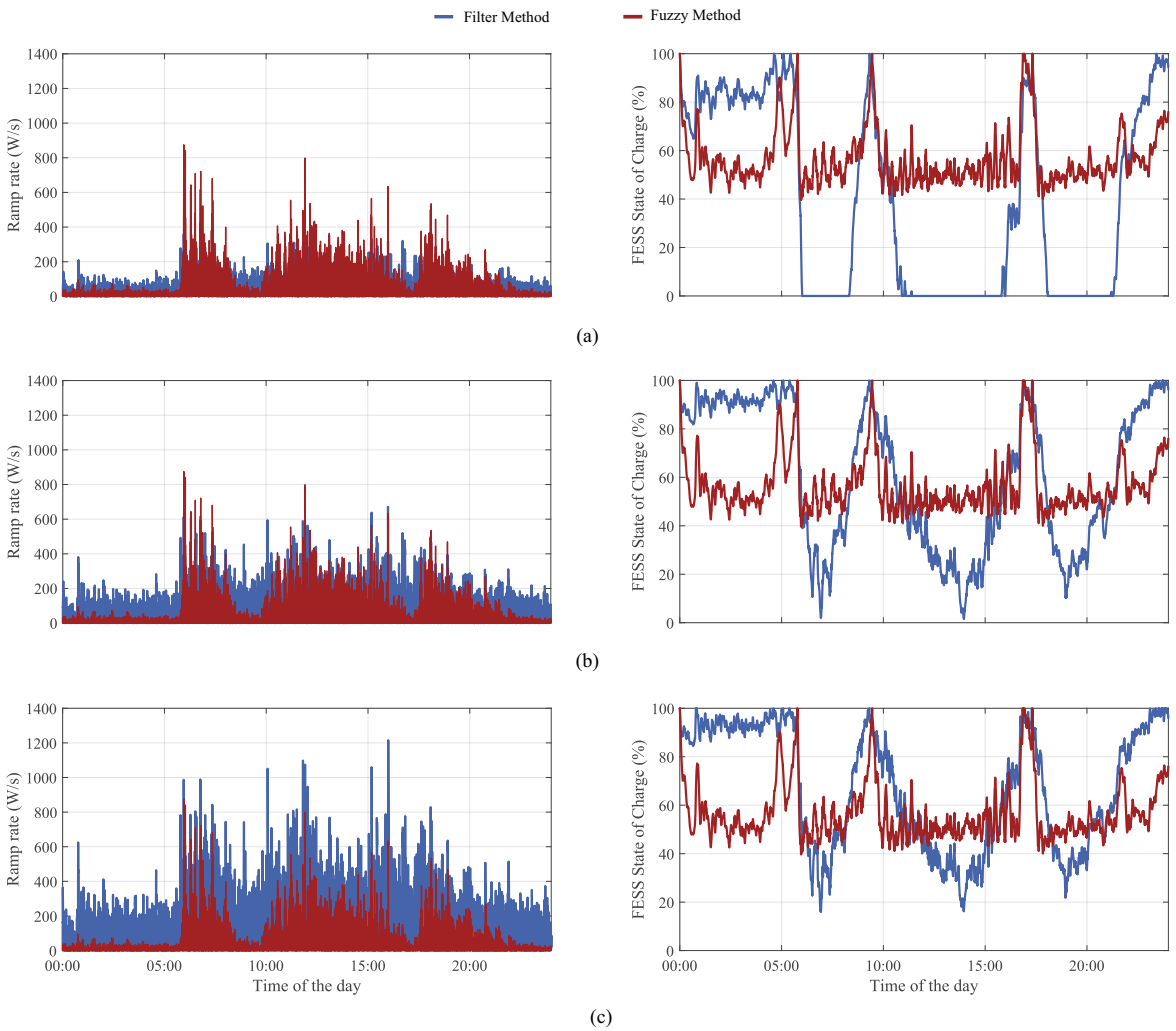

Fig. 15: Comparison of the different cut-off frequency (a) 1.5 mHz (b) 2.5 mHz (c) 3.5 mHZ

System (ESS) units based on their dynamic behavior. In addition, the integration of a Fuzzy Logic-based controller enables the minimization of the battery's ramp rate and facilitates the SoC correction for the flywheel. This dynamic reconfiguration of energy distribution guarantees harmonized ramp rates and SoC levels throughout the entire HESS, enabling the optimization of the trade-off between the battery's ramp rate and the flywheel's SoC.

REFERENCES

[1] J. Fang, Y. Tang, H. Li, and X. Li, "A battery/ultracapacitor hybrid energy storage system for implementing the power management of virtual synchronous generators," *IEEE Transactions on Power Electronics*, vol. 33, no. 4, pp. 2820–2824, 2018.

[2] C. Sun, S. Q. Ali, G. Joos, and F. Bouffard, "Design of hybrid-storage-based virtual synchronous machine with energy recovery control considering energy consumed in inertial and damping support," *IEEE Transactions on Power Electronics*, vol. 37, no. 3, pp. 2648–2666, 2022.

[3] D. Wang, S. Ge, H. Jia, C. Wang, Y. Zhou, N. Lu, and X. Kong, "A demand response and battery storage coordination algorithm for providing microgrid Tie-Line smoothing services," *IEEE Transactions on Sustainable Energy*, vol. 5, no. 2, pp. 476–486, 2014.

[4] R. Du, P. Zou, and C. Ma, "Multi-objective optimal sizing of hybrid energy storage systems for grid-connected wind farms using fuzzy control," *Journal of Renewable and Sustainable Energy*, vol. 13, no. 1, 2021.

[5] G. De Carne, A. Morandi, and S. Karrari, "Supercapacitor Modeling for Real-Time Simulation Applications," *IEEE Journal of Emerging and Selected Topics in Industrial Electronics*, vol. 3, no. 3, pp. 509–518, 2022.

[6] B. Sun, T. Dragičević, F. D. Freijedo, J. C. Vasquez, and J. M. Guerrero, "A control algorithm for electric vehicle fast charging stations equipped with flywheel energy storage systems," *IEEE Transactions on Power Electronics*, vol. 31, no. 9, pp. 6674–6685, 2016.

[7] A. S. Mir and N. Senroy, "Intelligently Controlled Flywheel Storage for Enhanced Dynamic Performance," *IEEE Transactions on Sustainable Energy*, vol. 10, no. 4, pp. 2163–2173, 2019.

[8] M. Ghanaatian and S. Lotfifard, "Control of Flywheel Energy Storage Systems in the Presence of Uncertainties," *IEEE Transactions on Sustainable Energy*, vol. 10, no. 1, pp. 36–45, 2019.

[9] F. Reißner and G. De Carne, "Virtual synchronous machine integration on a commercial flywheel for frequency grid support," *IEEE Transactions on Power Electronics*, vol. 39, no. 10, pp. 12086–12090, 2024.

[10] Beacon Power, "Stephentown, new york," 2018.

[11] Schwungrad Energie, "Rhode hybrid test facility," 2024.

[12] Amber Kinetics, Inc., "The world's only flywheel innovation hub," 2020.

[13] G. De Carne, S. M. Maroufi, H. Beiranvand, V. De Angelis, S. D'Arco, V. Gevorgian, S. Waczowicz, B. Mather, M. Liserre, and V. Hagenmeyer, "The role of energy storage systems for a secure energy supply: A comprehensive review of system needs and technology solutions," *Electric Power Systems Research*, vol. 236, p. 110963, 2024.

[14] Q. Xie, Y. Kim, Y. Wang, J. Kim, N. Chang, and M. Pedram, "Principles and efficient implementation of charge replacement in hybrid electrical energy storage systems," *IEEE Transactions on Power Electronics*, vol. 29, no. 11, pp. 6110–6123, 2014.

[15] L. Liu, D. Zhou, J. Zou, and Z. Shen, "Opposite vector modulation-based bidirectional power allocation for single-stage multiport inverter-connected hybrid energy storage system," *IEEE Transactions on Power Electronics*, vol. 39, no. 10, pp. 12200–12212, 2024.

[16] E. Wikner and T. Thiringer, "Extending battery lifetime by avoiding high soc," *Applied Sciences*, vol. 8, no. 10, 2018.

[17] K. Xu, Y. Guo, G. Lei, and J. Zhu, "A review of flywheel energy storage system technologies," *Energies*, vol. 16, no. 18, 2023.

[18] D. R. Conover, A. J. Crawford, V. V. Viswanathan, S. Ferreira, and D. Schoenwald, "Protocol for uniformly measuring and expressing the performance of energy storage systems," Tech. Rep. PNNL-22010 Rev 2/SAND2016-3078 R, Pacific Northwest National Laboratory, Richland, WA, USA, 2014.

[19] A. Khalid, A. Stevenson, and A. Sarwat, "Overview of technical specifications for grid-connected microgrid battery energy storage systems," *IEEE Access*, vol. PP, pp. 1–1, 12 2021.

[20] V. Muenzel, J. de Hoog, M. Brazil, A. Vishwanath, and S. Kalyanaraman, "A multi-factor battery cycle life prediction methodology for optimal battery management," 07 2015.

[21] S. Zhou, Z. Chen, D. Huang, and T. Lin, "Model prediction and rule based energy management strategy for a plug-in hybrid electric vehicle with hybrid energy storage system," *IEEE Transactions on Power Electronics*, vol. 36, no. 5, pp. 5926–5940, 2021.

[22] N. Omar, M. A. Monem, Y. Firouz, J. Salminen, J. Smekens, O. Hegazy, H. Gaulous, G. Mulder, P. Van den Bossche, T. Coosemans, and J. Van Mierlo, "Lithium iron phosphate based battery – assessment of the aging parameters and development of cycle life model," *Applied Energy*, vol. 113, pp. 1575–1585, 2014.

[23] W. Yanzi, X. Changle, and W. Wang, "Energy management strategy based on fuzzy logic for a new hybrid battery-ultracapacitor energy storage system," *IEEE Transportation Electrification Conference and Expo, ITEC Asia-Pacific 2014 - Conference Proceedings*, pp. 1–5, 2014.

[24] B. Wang, H. Fan, Z. Li, G. Feng, and Y. Han, "An Ultra-Local Model based Control Method with the Bus Voltage Supervisor for Hybrid Energy Storage System in Electric Vehicles," *IEEE Journal of Emerging and Selected Topics in Power Electronics*, vol. PP, pp. 1–1, 2023.

[25] S. T. Sisakat and S. M. Barakati, "Fuzzy energy management in electrical vehicles with different hybrid energy storage topologies," *4th Iranian Joint Congress on Fuzzy and Intelligent Systems, CFIS 2015*, pp. 10–15, 2016.

[26] O. Erdinc, B. Vural, and M. Uzunoglu, "A wavelet-fuzzy logic based energy management strategy for a fuel cell/battery/ultra-capacitor hybrid vehicular power system," *Journal of Power Sources*, vol. 194, no. 1, pp. 369–380, 2009.

[27] C. Balasundar, C. K. Sundarabalan, N. S. Srinath, J. Sharma, and J. M. Guerrero, "Interval Type2 Fuzzy Logic-Based Power Sharing Strategy for Hybrid Energy Storage System in Solar Powered Charging Station," *IEEE Transactions on Vehicular Technology*, vol. 70, no. 12, pp. 12450–12461, 2021.

[28] D. Xu and H. Cen, "A hybrid energy storage strategy based on multivariable fuzzy coordinated control of photovoltaic grid-connected power fluctuations," *IET Renewable Power Generation*, vol. 15, no. 8, pp. 1826–1835, 2021.

[29] S. Sinha and P. Bajpai, "Power management of hybrid energy storage system in a standalone DC microgrid," *Journal of Energy Storage*, vol. 30, no. May, 2020.

[30] D. Nderitu and P. V. Preckel, "Rachel Carnegie Douglas Gotham," no. June, 2013.

[31] H. H. Abdeltawab and Y. A. R. I. Mohamed, "Robust Energy Management of a Hybrid Wind and Flywheel Energy Storage System Considering Flywheel Power Losses Minimization and Grid-Code Constraints," *IEEE Transactions on Industrial Electronics*, vol. 63, no. 7, pp. 4242–4254, 2016.

[32] H. Garcia-Pereira, M. Blanco, G. Martinez-Lucas, J. I. Perez-Diaz, and J. I. Sarasua, "Comparison and Influence of Flywheels Energy Storage System Control Schemes in the Frequency Regulation of Isolated Power Systems," *IEEE Access*, vol. 10, pp. 37892–37911, 2022.

[33] M. S. Mahdavi, G. B. Gharehpetian, and H. A. Moghaddam, "Enhanced Frequency Control Method for Microgrid-Connected Flywheel Energy Storage System," *IEEE Systems Journal*, vol. 15, no. 3, pp. 4503–4513, 2020.

[34] S. Karrari, G. De Carne, and M. Noe, "Adaptive droop control strategy for Flywheel Energy Storage Systems: A Power Hardware-in-the-Loop validation," *Electric Power Systems Research*, vol. 212, no. April, 2022.

[35] K. Ding, F. Li, and X. Zhang, *Power Smoothing Control of DC Microgrid Hybrid Energy Storage System Based on Fuzzy Control*. 7 2019.

[36] J. Hou, Z. Song, H. F. Hofmann, and J. Sun, "Control Strategy for Battery/Flywheel Hybrid Energy Storage in Electric Shipboard Microgrids," *IEEE Transactions on Industrial Informatics*, vol. 17, no. 2, pp. 1089–1099, 2021.

[37] H. Biedka and K. Rafal, "Control Algorithms of Hybrid Energy Storage System Based on Fuzzy Logic," *2021 Progress in Applied Electrical Engineering, PAEE 2021*, pp. 10–14, 2021.

[38] R. J. Hyndman, "Moving averages," tech. rep., 2009.

[39] A. C. Szakmary, Q. Shen, and S. C. Sharma, "Trend-following trading strategies in commodity futures: A re-examination," *Journal of Banking and Finance*, vol. 34, no. 2, pp. 409–426, 2010.

[40] X. Liu, H. An, L. Wang, and Q. Guan, "Quantified moving average strategy of crude oil futures market based on fuzzy logic rules and genetic algorithms," *Physica A: Statistical Mechanics and its Applications*, vol. 482, pp. 444–457, 2017.

[41] E. H. Mamdani and S. Assilian, "An experiment in linguistic synthesis with a fuzzy logic controller," *International Journal of Man-Machine Studies*, vol. 7, no. 1, pp. 1–13, 1975.

[42] Z. Song, H. Hofmann, J. Li, J. Hou, X. Han, and M. Ouyang, "Energy management strategies comparison for electric vehicles with hybrid energy storage system," *Applied Energy*, vol. 134, pp. 321–331, 2014.

[43] S. Karrari, N. Ludwig, G. De Carne, and M. Noe, "Sizing of Hybrid Energy Storage Systems Using Recurring Daily Patterns," *IEEE Transactions on Smart Grid*, vol. 13, no. 4, pp. 3290–3300, 2022.

[44] S. Karrari, M. Vollmer, G. D. Carne, M. Noe, K. Böhm, and J. Geisbüsch, "A data-driven approach for estimating relative voltage sensitivity," in *2020 IEEE Power & Energy Society General Meeting (PESGM)*, pp. 1–5, 2020.

[45] A. Eberle GmbH & Co. KG, "Power quality-interface and disturbance recorder pqi-da smart." https://www.aeberle.de/en/product-groups/pq-fix-installed/devices/pqi-da-smart. [Online; accessed 2021-06-02].

[46] J. P. L. Keil, "Linear and Nonlinear Aging of Lithium-Ion Cells," 2021.

[47] F. Ashrafidehkordi, D. Kottonau, and G. De Carne, "Multi-Rate Discrete Domain Modeling of Power Hardware-in-The-Loop Setups," *IEEE Open Journal of Power Electronics*, vol. 4, no. July, pp. 539–548, 2023.

[48] P. Kotsampopoulos, D. Lagos, N. Hatziargyriou, M. O. Faruque, G. Lauss, O. Nzimako, P. Forsyth, M. Steurer, F. Ponci, A. Monti, V. Dinavahi, and K. Strunz, "A Benchmark System for Hardware-in-the-Loop Testing of Distributed Energy Resources," *IEEE Power and Energy Technology Systems Journal*, vol. 5, no. 3, pp. 94–103, 2018.

[49] S. Karrari, G. De Carne, and M. Noe, "Model validation of a high-speed flywheel energy storage system using power hardware-in-the-loop testing," *Journal of Energy Storage*, vol. 43, p. 103177, 2021.

[50] N. B. Lai, A. Tarraso, G. N. Baltas, L. V. Marin Arevalo, and P. Rodriguez, "External Inertia Emulation Controller for Grid-Following Power Converter," *IEEE Transactions on Industry Applications*, vol. 57, no. 6, pp. 6568–6576, 2021.

[51] J. Xiao, P. Wang, and L. Setyawan, "Hierarchical Control of Hybrid Energy Storage System in DC Microgrids," *IEEE Transactions on Industrial Electronics*, vol. 62, no. 8, pp. 4915–4924, 2015.

[52] T. Wu, W. Yu, and L. Guo, "A Study on Use of Hybrid Energy Storage System along with Variable Filter Time Constant to Smooth DC Power Fluctuation in Microgrid," *IEEE Access*, vol. 7, pp. 175377–175385, 2019.

[53] A. S. Gardouh, S. Abulanwar, F. Deng, E. Gouda, and A. Ghanem, "Novel fuzzy-based open-switch fault detection scheme of voltage source inverter induction motor drive," *IEEE Transactions on Power Electronics*, vol. 39, no. 11, pp. 14961–14973, 2024.

[54] V. Gurugubelli, A. Ghosh, A. K. Panda, and B. P. Behera, "Fuzzy-based adaptive voc methods for parallel inverters," *IEEE Transactions on Power Electronics*, vol. 39, no. 4, pp. 3956–3961, 2024.

[55] Y. Shen, J. Xie, T. He, L. Yao, and Y. Xiao, "Ceemd-fuzzy control energy management of hybrid energy storage systems in electric vehicles," *IEEE Transactions on Energy Conversion*, vol. 39, no. 1, pp. 555–566, 2024.

Seyede Masoome Marouf (Graduate Student Member, IEEE) received the B.Sc. degree in electrical engineering from the University of Guilan, Rasht, Iran, in 2016, and the M.Sc. degree cum laude in electrical engineering from the University of Bologna, Bologna, Italy, in 2020. During her master's studies, she participated in an Erasmus exchange at Aalborg University, Aalborg, Denmark, and conducted her master's thesis at the University of Florida, Gainesville, USA. She is currently pursuing the Ph.D. degree in control and power management of hybrid energy storage systems with the Real-Time System Integration Group, Energy Lab, Karlsruhe Institute of Technology, Karlsruhe, Germany. As part of her Ph.D., she completed a research period at University College Dublin, Dublin, Ireland. Her research interests include energy storage systems, power management, grid frequency and voltage control, power electronics integration in power systems, real-time simulations, and power hardware-in-the-loop.

Shahab Karrari received his B.Sc. and M.Sc. degrees in electrical power engineering from the Amirkabir University of Technology (Tehran Polytechnic), Tehran, Iran, in 2012 and 2014, respectively and the Ph.D. degree (summa cum laude) in integration of energy storage systems using real-time simulations from the Karlsruhe Institute for Technology (KIT), Karlsruhe, Germany, in 2021. Since 2022, he has been working as a Control Expert with Siemens Energy working on advanced grid support functionality of HVDC converter stations such as grid-forming control. His research interests include power system dynamics and control, energy storage systems, HVDC systems, grid-forming control, inertia emulation, and hardware-in-the-loop testing.

Karthik Rajashekaraiah received the B.Tech degree in Electrical & Electronics, and M.tech degree in Power Electronics from Visvesvaraya Institute of Technology, Belgaum, Karnataka, India in 2012, and 2016 respectively. He is currently pursuing his Ph.D. under Prof. Giovanni De Carne at Institute of Technical Physics (Energy Lab 2.0), Karlsruhe Institute of Technology, Karlsruhe, Germany. Previously, he worked as a Field Application Engineer with OPAL-RT Technologies India (P) Ltd., Bengaluru, India, from November 2016 to August 2021. Also, he worked as an Engineer Trainee at TeleDNA Communications India (P) Ltd., Bengaluru, India from September 2013 - September 2014. His research interests include modeling, simulation, and analysis of power electronics in power system applications, Power Hardware-in-the-Loop studies in real-time applications

Giovanni De Carne (Senior Member, IEEE) received the B.Sc. and M.Sc. degrees in electrical engineering from the Polytechnic University of Bari, Italy, in 2011 and 2013, respectively, and the Ph.D. degree from the Chair of Power Electronics, Kiel University, Germany, in 2018. Prof. De Carne is currently W3 (full) professor at the Institute for Technical Physics at the Karlsruhe Institute of Technology, Karlsruhe, Germany, where he leads the "Real Time Systems for Energy Technologies" Group and the "Power Hardware In the Loop Lab". He is currently supervising PhD students, managing academic and industrial projects, and developing multi-MW power hardware in the loop testing infrastructures for energy storage systems and hydrogen-based drives. He has authored/co-authored more than 100 peer-reviewed scientific papers. His research interests include power electronics integration in power systems, solid-state transformers, real-time modelling, and power hardware in the loop. Prof. De Carne successfully hosted the IEEE eGrid2023 Workshop in Karlsruhe in October 2023 with high participation from the industry. He has been the technical program committee chair for several IEEE conferences, and associate editor of the IEEE Open Journal of Power Electronics and several other IEEE and IET journals.